

## PAPER

# Joint MMSE-FDE & Spectrum Combining for a Broadband Single-Carrier Transmission in the Presence of Timing Offset

Tatsunori OBARA<sup>†a)</sup>, Kazuki TAKEDA<sup>†</sup>, *Student Members*, and Fumiyuki ADACHI<sup>†</sup>, *Fellow*

**SUMMARY** Frequency-domain equalization (FDE) based on minimum mean square error (MMSE) is considered as a promising equalization technique for a broadband single-carrier (SC) transmission. When a square-root Nyquist filter is used at a transmitter and receiver to limit the signal bandwidth, the presence of timing offset produces the inter-symbol interference (ISI) and degrades the bit error rate (BER) performance using MMSE-FDE. In this paper, we discuss the mechanism of the BER performance degradation in the presence of timing offset. Then, we propose joint MMSE-FDE & spectrum combining which can make use the excess bandwidth introduced by transmit filter to achieve larger frequency diversity gain while suppressing the negative effect of the timing offset.

**key words:** frequency-domain equalization, single-carrier transmission, Nyquist filter, timing offset, oversampling

## 1. Introduction

The broadband wireless channel is composed of many propagation paths with different time delays and the frequency-selective fading channel is produced [1]–[3]. Therefore, the bit error rate (BER) performance of the broadband single-carrier (SC) transmission degrades due to the strong inter-symbol interference (ISI). The use of the frequency-domain equalization (FDE) based on the minimum mean square error (MMSE) criterion can provide good BER performance [4]–[7]. However, this is only true in the case of no timing offset.

When a square-root Nyquist filter is used at a transmitter and a receiver to limit the signal bandwidth, the presence of timing offset between a transmitter and a receiver produces the ISI and degrades the BER performance. Recently, the impact of timing offset on the SC transmission using MMSE-FDE was discussed [8]–[10]. In [8] and [9], it was showed that when the timing offset exists, the BER performance degrades as the roll-off factor of Nyquist filter increases.

In this paper, we first discuss the mechanism that causes the BER performance degradation in the presence of timing offset. We show that when the timing offset is present, the spectrum distortion is produced since adjacent frequency-shifted spectra are given different phase rotations and overlapped if the roll-off factor of Nyquist filter is larger than 0. To solve this problem, we propose joint MMSE-FDE

& spectrum combining. In the proposed MMSE-FDE, first, the received signal is oversampled at 2 times higher rate than the symbol rate. Then, joint MMSE-FDE & spectrum combining is applied to simultaneously compensate for both the phase rotation due to the timing offset and the spectrum distortion due to the channel frequency-selectivity. As the roll-off factor increases, larger frequency diversity gain can be achieved and the BER performance can be improved.

The remainder of this paper is organized as follows. In Sect. 2, we discuss the impact of the timing offset on the SC transmission using the conventional MMSE-FDE. In Sect. 3, joint MMSE-FDE & spectrum combining is proposed. In Sect. 4, we evaluate the BER performance of the SC transmission using the conventional MMSE-FDE in the presence of timing offset and the effect of the proposed MMSE-FDE by computer simulation. Section 5 concludes this paper.

## 2. Conventional MMSE-FDE in the Presence of Timing Offset

### 2.1 System Model

The system model of the SC transmission using the conventional MMSE-FDE is illustrated in Fig. 1. At the transmitter, the binary information sequence is data-modulated, and then the symbol sequence is divided into a sequence of  $N_c$ -symbol blocks, where  $N_c$  is the size of fast Fourier transform (FFT).  $N_g$ -symbol cyclic prefix (CP) is inserted into the guard interval (GI) of each symbol-block. The GI-inserted symbol block is transmitted after passing through

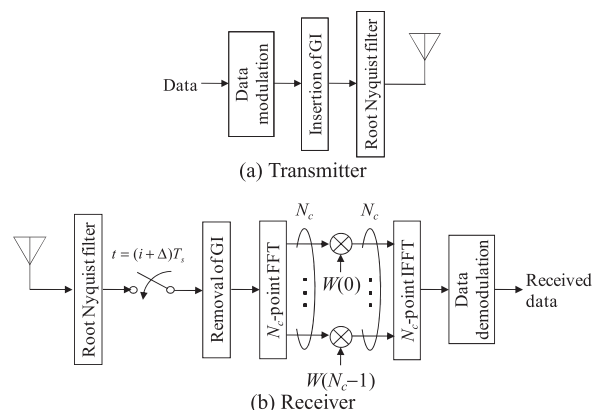


**Fig. 1** System model of SC transmission using the conventional MMSE-FDE.

Manuscript received December 22, 2009.

Manuscript revised October 20, 2010.

<sup>†</sup>The authors are with the Department of Electrical and Communication Engineering, Graduate School of Engineering, Tohoku University, Sendai-shi, 980-8579 Japan.

a) E-mail: obara@mobile.ecei.tohoku.ac.jp

DOI: 10.1587/transcom.E94.B.1366

the square-root Nyquist transmit filter to limit the signal bandwidth.

The transmitted symbol block is received via a frequency-selective fading channel. The received sequence passes through the square-root Nyquist receive filter and is sampled at the symbol rate  $1/T_s$ . After the GI removal, the received symbol block is transformed into the frequency-domain signal by  $N_c$ -point FFT. Then, one-tap MMSE-FDE is carried out on the frequency-domain received signal. The frequency-domain signal after MMSE-FDE is transformed by  $N_c$ -point inverse FFT (IFFT) into the time-domain signal.

## 2.2 Signal Representation

The transmitted signal  $s(n)$  can be expressed as

$$s(n) = \sum_{m=-\infty}^{\infty} s_m(n - m(N_c + N_g)), \quad (1)$$

where  $s_m(n)$  is the  $m$ th GI-inserted symbol block expressed as

$$s_m(n) = \begin{cases} d_m(n \bmod N_c), & -N_g \leq n < N_c - 1 \\ 0, & \text{elsewhere} \end{cases}, \quad (2)$$

where  $\{d_m(n); n = 0 \sim N_c - 1\}$  is the data-modulated symbol sequence. The symbol sequence after passing through the transmit filter is expressed as

$$s_T(t) = \sqrt{\frac{2E_s}{T_s}} \sum_{n=-\infty}^{\infty} s(n)\varphi(t - n), \quad (3)$$

where  $E_s$  and  $T_s$  are the symbol energy and the symbol duration, respectively, and  $\varphi_T(t)$  is the impulse response of the transmit filter.

The transmitted signal is received via a frequency-selective fading channel. The received signal  $r_X(t)$  can be expressed as

$$r_X(t) = \int_{-\infty}^{\infty} s_T(\tau)h_c(t - \tau)d\tau, \quad (4)$$

where  $h_c(t)$  is the channel impulse response given by

$$h_c(t) = \sum_{l=0}^{L-1} h_l\delta(t - \tau_l), \quad (5)$$

where  $h_l$  and  $\tau_l$  are the complex-valued path gain and the delay time of the  $l$ th path ( $l = 0 \sim L - 1$ ), respectively. The received signal after passing through the receive filter can be expressed as

$$r_R(t) = \sqrt{\frac{2E_s}{T_s}} \sum_{n=-\infty}^{\infty} s(n)h(t - n) + \eta_R(t), \quad (6)$$

where  $h(t)$  is the impulse response of the composite channel (transmit filter + channel + receive filter), and  $\eta_R(t)$  is the

filter output of the additive white Gaussian noise (AWGN).  $h(t)$  is given as

$$h(t) = \sum_{l=0}^{L-1} h_l\varphi(t - \tau_l), \quad (7)$$

where  $\varphi(t)$  denotes the the impulse response of the overall (transmit and receive) filter. In this paper, we assume that the raised cosine filter is used as the overall filter.  $\varphi(t)$  is expressed as [2], [3]

$$\varphi(t) = \frac{\sin \pi t}{\pi t} \frac{\cos \alpha \pi t}{1 - (2\alpha t)^2}. \quad (8)$$

where  $\alpha$  is the roll-off factor.

$r_R(t)$  is sampled at the symbol rate  $1/T_s$ . Without loss of generality, we consider the reception of the  $m = 0$ th transmitted symbol block. The sampled symbol sequence  $\{r(i); i = 0 \sim N_c - 1\}$  after GI removal can be expressed as

$$\begin{aligned} r(i) &= r_R(i + \Delta) \\ &= \sqrt{\frac{2E_s}{T_s}} \sum_{l'=-\infty}^{\infty} h(l' + \Delta)s_0((i - l') \bmod N_c) \\ &\quad + \nu(i) + \eta(i), \end{aligned} \quad (9)$$

where  $\Delta$  denotes the timing offset normalized by  $T_s$  and  $\nu(i)$  and  $\eta(i)$  are the inter-block interference (IBI) and the noise with zero mean and variance  $2N_0/T_s$  with  $N_0$  being the single-sided power spectrum density, respectively.  $\nu(i)$  is given by [11]

$$\begin{aligned} \nu(i) &= \sqrt{\frac{2E_s}{T_s}} \sum_{l'=-\infty}^{-1} h(l' + \Delta) \\ &\quad \times \{s(i - l') - s_0((i - l') \bmod N_c)\} \\ &\quad \times u(i - N_c - l') \\ &\quad + \sqrt{\frac{2E_s}{T_s}} \sum_{l'=0}^{\infty} h(l' + \Delta) \\ &\quad \times \{s(i - l') - s_0((i - l') \bmod N_c)\} \\ &\quad \times \{u(i) - u(i + N_g - l')\}, \end{aligned} \quad (10)$$

where  $u(i) = 1(0)$  for  $i \geq 0$  ( $i < 0$ ).

An  $N_c$ -point FFT is applied to  $\{r(i); i = 0 \sim N_c - 1\}$  to transform it into the frequency-domain signal  $\{R(k); k = -N_c/2 \sim N_c/2 - 1\}$ .  $R(k)$  is given by

$$\begin{aligned} R(k) &= \frac{1}{\sqrt{N_c}} \sum_{i=0}^{N_c-1} r(i) \exp\left(-j2\pi k \frac{i}{N_c}\right) \\ &= \sqrt{\frac{2E_s}{T_s}} H(k, \Delta)S(k) + N(k) + \Pi(k), \end{aligned} \quad (11)$$

where  $H(k, \Delta)$ ,  $S(k)$ ,  $N(k)$  and  $\Pi(k)$  are the overall (transmit/receive filter + channel) transfer function, the signal, the IBI and the noise component at  $k$ th frequency, respectively, as

$$\begin{cases} S(k) = \frac{1}{\sqrt{N_c}} \sum_{i=0}^{N_c-1} s_0(i) \exp\left(-j2\pi k \frac{i}{N_c}\right) \\ H(k, \Delta) = \sum_{l'=-\infty}^{\infty} h(l' + \Delta) \exp\left(-j2\pi k \frac{l'}{N_c}\right) \\ N(k) = \frac{1}{\sqrt{N_c}} \sum_{i=0}^{N_c-1} v(i) \exp\left(-j2\pi k \frac{i}{N_c}\right) \\ \Pi(k) = \frac{1}{\sqrt{N_c}} \sum_{i=0}^{N_c-1} \eta(i) \exp\left(-j2\pi k \frac{i}{N_c}\right) \end{cases}, \quad (12)$$

One-tap MMSE-FDE is carried out on  $R(k)$  as

$$\begin{aligned} \hat{R}(k) &= R(k)W(k) \\ &= \sqrt{\frac{2E_s}{T_s}} \hat{H}(k, \Delta) S(k) + \hat{N}(k) + \hat{\Pi}(k), \end{aligned} \quad (13)$$

where  $\hat{H}(k, \Delta)$ ,  $\hat{N}(k)$  and  $\hat{\Pi}(k)$  are the equivalent channel gain, the IBI and the noise after MMSE-FDE, respectively, as

$$\begin{cases} \hat{H}(k, \Delta) = W(k)H(k, \Delta) \\ \hat{N}(k) = W(k)N(k) \\ \hat{\Pi}(k) = W(k)\Pi(k) \end{cases}, \quad (14)$$

$W(k)$  is the MMSE-FDE weight expressed as [7]

$$W(k) = \frac{H^*(k, \Delta)}{|H(k, \Delta)|^2 + \Lambda^{-1}(\Delta)}, \quad (15)$$

where  $\Lambda(\Delta)$  denotes the signal-to-interference plus noise power ratio (SINR) and is given by

$$\Lambda(\Delta) = \frac{1}{\left[ \left( \frac{E_s}{N_0} \right)^{-1} + \frac{2}{N_c} \sum_{l'=-\infty}^{-1} |h(l' + \Delta)|^2 |l'| + \frac{2}{N_c} \sum_{l'=N_g}^{\infty} |h(l' + \Delta)|^2 (l' - N_g) \right]}, \quad (16)$$

$H(k, \Delta)$  can be estimated by using pilot-assisted channel estimation [12]–[14]. In this paper, ideal channel estimation is assumed. The equalized frequency-domain signal  $\hat{R}(k)$ ;  $k = -N_c/2 \sim N_c/2 - 1$  is transformed by an  $N_c$ -point IFFT into the time-domain signal  $\hat{r}(i)$ ;  $i = 0 \sim N_c - 1$ .

### 2.3 Spectrum Distortion due to Timing Offset

$H(k, \Delta)$  can be rewritten as (see Appendix A)

$$\begin{aligned} H(k, \Delta) &= \sum_{l'=-\infty}^{\infty} H_c(k - l'N_c) \Phi(k - l'N_c) \\ &\quad \times \exp\left\{j2\pi(k - l'N_c) \frac{\Delta}{N_c}\right\}, \end{aligned} \quad (17)$$

where  $H_c(k)$  and  $\Phi(k)$  are respectively the channel gain at  $k$ th frequency and the transfer function of the overall (transmit + receive) filter.  $H_c(k)$  and  $\Phi(k)$  are respectively given

as

$$H_c(k) = \sum_{l=0}^{L-1} h_l \exp\left(-j2\pi k \frac{\tau_l}{N_c}\right), \quad (18)$$

$$\Phi(k) = \begin{cases} 1, & 0 \leq \left| \frac{k}{N_c} \right| \leq \frac{1-\alpha}{2} \\ \cos^2 \frac{\pi}{2\alpha} \left( \left| \frac{k}{N_c} \right| - \frac{1-\alpha}{2} \right), & \frac{1-\alpha}{2} \leq \left| \frac{k}{N_c} \right| \leq \frac{1+\alpha}{2} \\ 0, & \text{elsewhere} \end{cases}. \quad (19)$$

To discuss the impact of timing offset, we consider the flat fading channel case ( $H_c(k) = 1$  for all  $k$ ). In this case,  $H(k, \Delta)$  can be rewritten as

$$\begin{aligned} H(k, \Delta) &= \sum_{l'=-\infty}^{\infty} \Phi(k - l'N_c) \exp\left\{j2\pi(k - l'N_c) \frac{\Delta}{N_c}\right\} \\ &\equiv \tilde{\Phi}(k, \Delta), \end{aligned} \quad (20)$$

If  $\Delta = 0$  (no timing offset case),  $\tilde{\Phi}(k, \Delta)$  becomes unity for all  $k$ . The received signal spectrum after the symbol rate sampling is the sum of the copies of the original spectrum, each copy being frequency-shifted by an integer multiple of the sampling rate. The adjacent frequency-shifted spectra overlap when  $\alpha > 0$  as shown in Fig. 2. If the timing offset is not present, the signal spectrum whose amplitude is unity is recovered over the frequency range of  $-N_c/2 \leq k < N_c/2$ . On the other hand, if the timing offset is present, each frequency-shifted spectrum is phase-rotated (see Eq. (20)) and therefore, the spectrum over the overlapped interval is distorted since the adjacent frequency-shifted spectra are given different phase rotation. In Fig. 3, the value of  $\tilde{\Phi}(k, \Delta)$  in the case of  $\alpha = 0.5$  is plotted as the function of frequency index  $k$ . If  $\Delta = 0$  (no timing offset case),  $\tilde{\Phi}(k, \Delta) = 1 + j0$  irrespective of  $k$ . However, when the timing offset is present,  $\tilde{\Phi}(k, \Delta) \neq 1 + j0$  since each frequency-shifted spectrum is phase-rotated due to the timing offset.

Figure 4 plots the value of  $|\tilde{\Phi}(k, \Delta)|$  with  $\alpha$  as a parameter when  $\Delta = 0.5$ . When  $\alpha = 0$ ,  $|\tilde{\Phi}(k, \Delta)| = 1$  at all  $k$  since the frequency-shifted spectra which is phase-rotated due to the timing offset do not overlap. Therefore, even if the timing offset exists, the BER performance does not degrade when  $\alpha = 0$ . On the other hand, when  $\alpha > 0$ ,  $|\tilde{\Phi}(k, \Delta)|$  drops in the overlapped interval due to the phase rotation. As  $\alpha$  increases, the overlapped interval becomes wider and

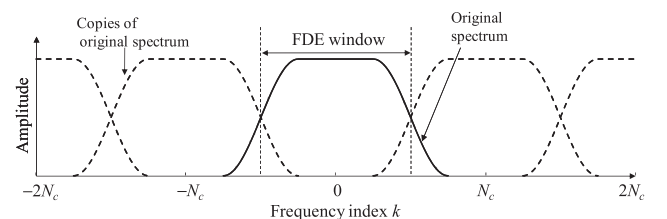
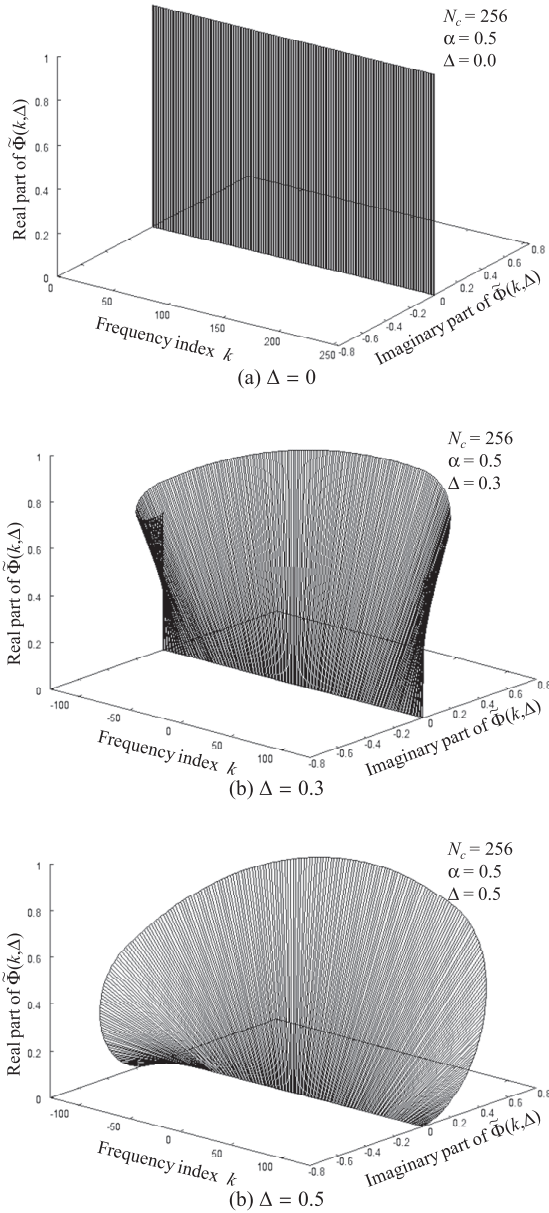


Fig. 2 Signal spectrum after symbol-rate sampling.



**Fig. 3** Observation of  $\tilde{\Phi}(k, \Delta)$  for  $\alpha = 0.5$ .

the spectrum distortion becomes larger.

Figure 5 plots the one-shot observation of the original channel gain  $H_c(k)$  and the equivalent channel gain  $\hat{H}(k, \Delta)$  after the MMSE-FDE when  $\delta = 0.5$  with  $\alpha$  as a parameter. It is seen from Fig. 5 that, as  $\alpha$  increases, the spectrum distortion becomes stronger due to the overlapping of adjacent frequency-shifted spectra which are given different phase rotations due to the timing offset, thereby degrading the BER performance.

### 3. Joint MMSE-FDE & Spectrum Combining

When the timing offset is present, the spectrum distortion is produced since adjacent frequency-shifted spectra are given different phase rotations and overlapped if  $\alpha > 0$ . To solve

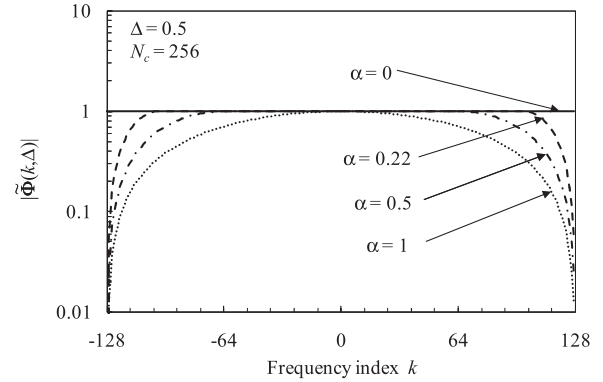


**Fig. 4** Amplitude of  $\tilde{\Phi}(k, \Delta)$ .

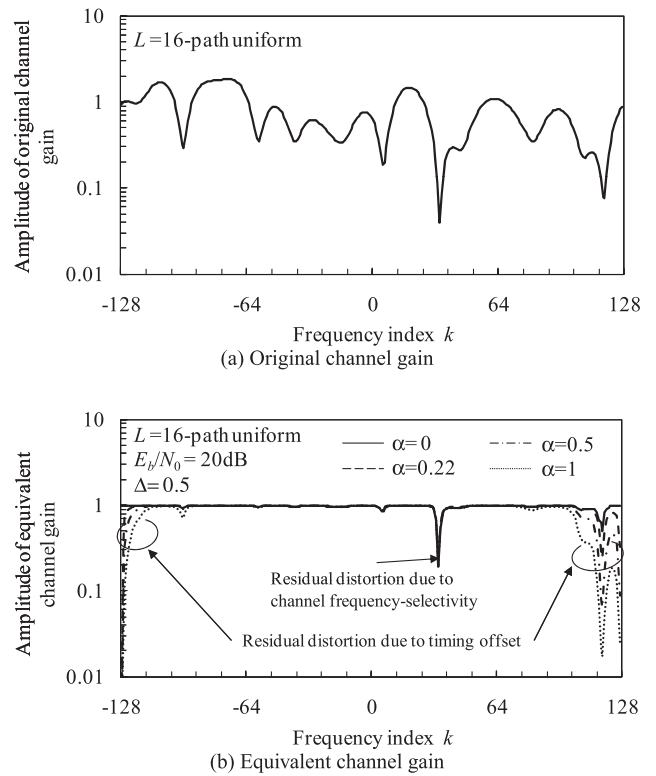


**Fig. 5** One-shot observation of equivalent channel gain.

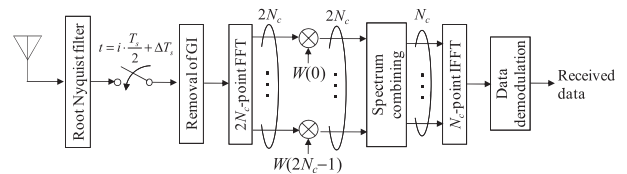


**Fig. 6** Receiver structure using joint MMSE-FDE & spectrum combining.

this problem, we propose joint MMSE-FDE & spectrum combining. In Fig. 6, the receiver structure of the SC transmission using joint MMSE-FDE & spectrum combining is illustrated. First, the received signal is oversampled at a rate faster than the symbol rate to avoid the spectrum overlap-

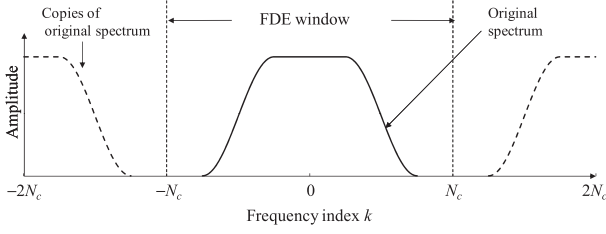


Fig. 7 Signal spectrum after double oversampling.

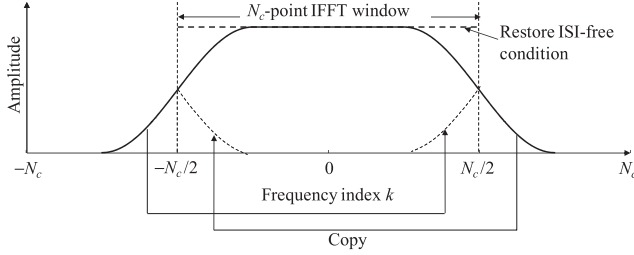


Fig. 8 Spectrum combining.

ping. When the square-root raised cosine filter is used as the transmit and receive filters, the spectrum overlapping can be avoided by using double oversampling (the received signal sampled at the rate  $2/T_s$ ) as shown in Fig. 7. Then, the simultaneous compensation of both the phase rotation due to the timing offset and the spectrum distortion due to the channel frequency-selectivity and the spectrum combining (or the frequency-domain down sampling) based on the MMSE criterion are performed (this is called joint MMSE-FDE & spectrum combining) as shown in Fig. 8 to recover the ISI-free condition over the desired frequency range of  $-N_c/2 \leq k < N_c/2$ . The frequency-domain signal after joint MMSE-FDE & spectrum combining is transformed by an  $N_c$ -point IFFT into the time-domain signal.

### 3.1 Signal Representation

The output of the receive filter is sampled at the rate  $2/T_s$ . The oversampled signal  $r(i); i = 0 \sim 2N_c - 1$  after the removal of a  $2N_g$ -sample GI can be expressed as

$$\begin{aligned}
 r(i) &= r_R\left(\frac{i}{2} + \Delta\right) \\
 &= \sqrt{\frac{2E_s}{T_s}} \sum_{n=-\infty}^{\infty} s_0(n \bmod N_c) h\left(\frac{i}{2} + \Delta - n\right) \\
 &\quad + v(i) + \eta_R\left(\frac{i}{2} + \Delta\right) \\
 &= \sqrt{\frac{2E_s}{T_s}} \sum_{l'=-\infty}^{\infty} h\left(\frac{l'}{2} + \Delta\right) \tilde{s}_0((i - l') \bmod 2N_c) \\
 &\quad + v(i) + \eta(i),
 \end{aligned} \tag{21}$$

where

$$\tilde{s}_m(i) = \begin{cases} s_m(n), & i = 2n \\ 0, & \text{else} \end{cases}. \tag{22}$$

In Eq. (21),  $\eta(i) = \eta_R(i/2 + \Delta)$  is the oversampled noise component.  $v(i)$  is the IBI component given by

$$\begin{aligned}
 v(i) &= \sqrt{\frac{2E_s}{T_s}} \sum_{l'=-\infty}^{-1} h\left(\frac{l'}{2} + \Delta\right) \\
 &\quad \times \{s(i - l') - s_0((i - l') \bmod 2N_c)\} \\
 &\quad \times u(i - 2N_c - l') \\
 &\quad + \sqrt{\frac{2E_s}{T_s}} \sum_{l'=0}^{\infty} h\left(\frac{l'}{2} + \Delta\right) \\
 &\quad \times \{s(i - l') - s_0((i - l') \bmod 2N_c)\} \\
 &\quad \times \{u(i) - u(i + 2N_g - l')\},
 \end{aligned} \tag{23}$$

where

$$\tilde{s}(i) = \sum_{m=-\infty}^{\infty} \tilde{s}_m(i - m(2N_g + 2N_c)), \tag{24}$$

A  $2N_c$ -point FFT is applied to transform the oversampled signal block  $\{r(i); i = 0 \sim 2N_c - 1\}$  into the frequency-domain signal  $\{R(k); k = -N_c \sim N_c - 1\}$ . The  $k$ th frequency component  $R(k)$  can be expressed as

$$\begin{aligned}
 R(k) &= \frac{1}{\sqrt{2N_c}} \sum_{i=0}^{2N_c-1} r(i) \exp\left(-j2\pi k \frac{i}{2N_c}\right) \\
 &= \sqrt{\frac{2E_s}{T_s}} H(k, \Delta) S(k) + N(k) + \Pi(k),
 \end{aligned} \tag{25}$$

where  $H(k, \Delta)$ ,  $S(k)$ ,  $N(k)$  and  $\Pi(k)$  are the composite (transmit/receive + channel) transfer function, the signal component, the IBI component, and the noise component, respectively.  $S(k)$  and  $H(k, \Delta)$  are given by

$$\begin{cases} S(k) = \frac{1}{\sqrt{2N_c}} \sum_{i=0}^{2N_c-1} \tilde{s}_0(i) \exp\left(-j2\pi k \frac{i}{2N_c}\right) \\ = \frac{1}{\sqrt{2N_c}} \sum_{i=0}^{N_c-1} s_0(i) \exp\left(-j2\pi k \frac{i}{N_c}\right) \\ H(k, \Delta) = \sum_{l'=-\infty}^{\infty} h\left(\frac{l'}{2} + \Delta\right) \exp\left(-j2\pi k \frac{l'}{2N_c}\right) \end{cases} \tag{26}$$

where  $H(k, \Delta)$  can be rewritten as

$$\begin{aligned}
 H(k, \Delta) &= \sum_{l'=-\infty}^{\infty} H_c(k - 2l'N_c) \Phi(k - 2l'N_c) \\
 &\quad \times \exp\left\{j2\pi(k - 2l'N_c) \frac{\Delta}{N_c}\right\}.
 \end{aligned} \tag{27}$$

From Eq. (27), it can be understood that the copies of the original spectrum are frequency-shifted by integer multiple of  $2/T_s$  and do not overlap even if  $\alpha > 0$ . Therefore, the spectrum is not distorted at all due to the timing offset.

### 3.2 Joint FDE & Spectrum Combining

The frequency-domain signal  $\{\hat{R}(k); k = -N_c/2 \sim N_c/2 - 1\}$

after joint MMSE-FDE & spectrum combining is given by

$$\begin{aligned}\hat{R}(k) &= \sum_{q=-1}^1 R(k - qN_c)W(k - qN_c) \\ &= \sqrt{\frac{2E_s}{T_s}} \hat{H}(k, \Delta)S(k) + \hat{N}(k) + \hat{\Pi}(k)\end{aligned}\quad (28)$$

where

$$\begin{cases} \hat{H}(k, \Delta) = \sum_{q=-1}^1 H(k - qN_c, \Delta)W(k - qN_c) \\ \hat{N}(k) = \sum_{q=-1}^1 N(k - qN_c)W(k - qN_c) \\ \hat{\Pi}(k) = \sum_{q=-1}^1 \Pi(k - qN_c)W(k - qN_c) \end{cases} \quad (29)$$

In Eq. (28),  $W(k)$  is the MMSE weight which simultaneously compensates the phase rotation due to the timing offset and the spectrum distortion due to the channel frequency-selectivity.

The frequency-domain signal  $\{\hat{R}(k); k = -N_c/2 \sim N_c/2 - 1\}$  after joint MMSE-FDE & spectrum combining is transformed by an  $N_c$ -point IFFT into the time-domain signal  $\{\hat{r}(i); i = 0 \sim N_c - 1\}$  for succeeding data demodulation as

$$\hat{r}(i) = \frac{1}{\sqrt{N_c}} \sum_{k=-N_c/2}^{N_c/2-1} \hat{R}(k) \exp\left(j2\pi i \frac{k}{N_c}\right). \quad (30)$$

In the following, we derive the MMSE weight  $W(k)$ .

We define the equalization error  $e(k)$  after FDE and spectrum combining over  $-N_c/2 \leq k < N_c/2$  as

$$\begin{aligned}e(k) &= \hat{R}(k) - \sqrt{\frac{2E_s}{T_s}} S(k) \\ &= \sum_{q=-1}^1 R(k - qN_c)W(k - qN_c) - \sqrt{\frac{2E_s}{T_s}} S(k).\end{aligned}\quad (31)$$

The MMSE weight  $W(k)$  which minimizes the MSE  $E[|e(k)|^2]$  of  $e(k)$  can be derived as (see Appendix B) [15]

$$W(k) = \frac{H^*(k, \Delta)}{\sum_{q=-1}^1 \frac{\Lambda^{-1}(k, \Delta)}{\Lambda^{-1}(k - qN_c, \Delta)} |H(k - qN_c, \Delta)|^2 + \Lambda^{-1}(k, \Delta)} \quad (32)$$

where  $\Lambda(k, \Delta)$  denotes the SINR at the  $k$ th frequency given by

$$\Lambda(k, \Delta) = \frac{1}{\left[ \left( \frac{E_s}{N_0} \right)^{-1} \Phi(k) + \frac{2}{N_c} \sum_{l'=-\infty}^{-1} \left| h\left( \frac{l'}{2} + \Delta \right) \right|^2 |l'| + \frac{2}{N_c} \sum_{l'=2N_g}^{\infty} \left| h\left( \frac{l'}{2} + \Delta \right) \right|^2 (l' - 2N_g) \right]}. \quad (33)$$

Since the IBI power is much smaller than the signal power,  $\Lambda(k, \Delta)$  can be approximated as  $\Lambda(k, \Delta) \approx (E_s/N_0)\Phi^{-1}(k)$ . Therefore, the MMSE weight of Eq. (32) can be approximated as

$$W(k) \approx \frac{H_c^*(k) \exp(j2\pi k \Delta / N_c)}{\sum_{q=-1}^1 |H_c(k - qN_c)|^2 + \left( \frac{E_s}{N_0} \right)^{-1}} \quad (34)$$

The  $k$ th frequency component after joint MMSE-FDE & spectrum combining is the weighted sum of  $R(k)$  and  $R(k - N_c)$  for  $k = 0 \sim N_c/2 - 1$ , and is the weighted sum of  $R(k)$  and  $R(k + N_c)$  for  $k = -N_c/2 \sim -1$ . For the no timing offset case ( $\Delta = 0$ ),  $W(k)$ ,  $W(k - N_c)$ , and  $W(k + N_c)$  can be given as

$$\begin{cases} W(k) \approx \begin{cases} \frac{H_c^*(k)}{|H_c(k)|^2 + |H_c(k - N_c)|^2 + \left( \frac{E_s}{N_0} \right)^{-1}} & \text{for } k = 0 \sim \frac{N_c}{2} - 1 \\ \frac{H_c^*(k)}{|H_c(k)|^2 + |H_c(k + N_c)|^2 + \left( \frac{E_s}{N_0} \right)^{-1}} & \text{for } k = -\frac{N_c}{2} \sim -1 \end{cases} \\ W(k - N_c) \approx \frac{H_c^*(k - N_c)}{|H_c(k)|^2 + |H_c(k - N_c)|^2 + \left( \frac{E_s}{N_0} \right)^{-1}} & \text{for } k = 0 \sim \frac{N_c}{2} - 1 \\ W(k + N_c) \approx \frac{H_c^*(k + N_c)}{|H_c(k)|^2 + |H_c(k + N_c)|^2 + \left( \frac{E_s}{N_0} \right)^{-1}} & \text{for } k = -\frac{N_c}{2} \sim -1 \end{cases} \quad (35)$$

which are the same MMSE weights of joint MMSE-FDE & antenna diversity combining (see Eq. (27) of [7]). When  $|H_c(k)|^2, |H_c(k - N_c)|^2, |H_c(k + N_c)|^2 \ll (E_s/N_0)^{-1}$ , Eq. (35) can be further approximated as

$$\begin{cases} W(k) \propto H_c^*(k) \\ W(k - N_c) \propto H_c^*(k - N_c) \\ W(k + N_c) \propto H_c^*(k + N_c) \end{cases} \quad (36)$$



This suggests that when the channel gain drops, the MMSE weight of Eq. (32) approximately acts as the maximal ratio combining (MRC) weight.

#### 4. Computer Simulation

We show the computer simulation results. The simulation condition is summarized in Table 1. We assume quadrature phase shift keying (QPSK) modulation, a signal block length of  $N_c = 256$  symbols and a GI length of  $N_g = 32$  symbols. The propagation channel is assumed to be a  $T_s/2$ -spaced  $L = 32$ -path frequency-selective block Rayleigh fading channel having uniform power delay profile. The timing offset  $\Delta$  is assumed to be uniformly distributed over  $[-0.5, 0.5]$ . The ideal channel estimation is also assumed.

Figure 9 plots the BER performance of the proposed joint MMSE-FDE & spectrum combining as a function of the roll-off factor  $\alpha$  when the average received bit energy-to-noise power spectrum density ratio  $E_b/N_0 (= 0.5(E_s/N_0)(1 + N_g/N_c)) = 12$  dB. For comparison, the performance of the conventional MMSE-FDE and that of MMSE-FDE with spectrum combining using the weight which minimizes the equalization error before spectrum combining is also plotted. The MMSE weight of MMSE-FDE with spectrum combining minimizes the equalization error  $e(k) = R(k)W(k) -$

$\sqrt{2E_s/T_s}\Phi(k)S(k)$  before spectrum combining and is given by

$$W(k) = \frac{H^*(k, \Delta)\Phi(k)}{|H(k, \Delta)|^2 + \Lambda^{-1}(k, \Delta)} \quad (37)$$

As shown in Fig. 9, when the timing offset exists, the performance of the conventional MMSE-FDE degrades as  $\alpha$  increases. On the other hand, both the proposed joint MMSE-FDE & spectrum combining and MMSE-FDE with spectrum combining achieve almost the same performance as in the no timing offset case irrespective of  $\alpha$ . The performances of both joint MMSE-FDE & spectrum combining and MMSE-FDE with spectrum combining improve as  $\alpha$  increases. The reason for this is that, as the signal bandwidth becomes wider, the proposed joint MMSE-FDE & spectrum combining and MMSE-FDE with spectrum combining can achieve increased frequency diversity gain due to joint equalization and frequency diversity combining. Note that if the channel has symbol-spaced time delays, the frequency diversity gain does not depend on the value of  $\alpha$  since the channel transfer function is a periodic function of period  $N_c/T_s$ . As seen from Fig. 9, the joint MMSE-FDE & spectrum combining provides much better performance than MMSE-FDE with spectrum combining. This is because the spectrum combining is similar to equal-gain diversity combining in MMSE-FDE with spectrum combining, while it is similar to maximal ratio combining in joint MMSE-FDE & spectrum combining.

Figure 10 plots the average BER performance as a function of  $E_b/N_0$  with  $\alpha$  as a parameter. As shown in Fig. 10(a), when  $\alpha = 0$ , the conventional MMSE-FDE in the presence of timing offset achieves almost the same performance as in the no timing offset case. This is because the adjacent spectra, which are phase-rotated due to the timing offset, do not overlap and therefore, no spectrum distortion is produced. However, as  $\alpha$  increases, the performance of the conventional MMSE-FDE degrades since the residual spectrum distortion becomes severer due to the overlapping of adjacent spectra which are given different phase rotations due to the timing offset. On the other hand, the proposed joint MMSE-FDE & spectrum combining can achieve almost the same performance as in the no timing offset case irrespective of  $\alpha$  since the overlapping of the phase-rotated spectra can be avoided by double oversampling and the phase rotation can be compensated by FDE. As  $\alpha$  increases, the use of joint MMSE-FDE & spectrum combining achieves much better performance than the conventional MMSE-FDE since the signal bandwidth becomes wider and larger frequency diversity gain can be achieved. The required  $E_b/N_0$  for BER =  $10^{-3}$  in the presence of timing offset can be reduced by about 3 and 6.8 dB from that of the conventional MMSE-FDE when  $\alpha = 0.5$  and 1, respectively.

Table 1 Simulation condition.

Data modulation	QPSK	
Transmitter	Block length	$N_c=256$
	GI length	$N_g=32$
Channel	Frequency-selective block Rayleigh fading	
	Power delay profile	$L=32$ -path uniform
Nyquist filter	Raised cosine filter	
	Roll-off factor	$\alpha=0\sim 1$
Receiver	Timing offset	$\Delta \in [-0.5, 0.5]$
	Channel estimation	Ideal

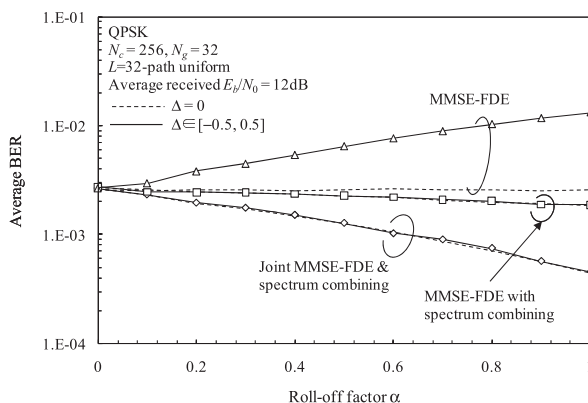


Fig. 9 Impact of  $\alpha$ .

#### 5. Conclusion

In this paper, we clarified the mechanism that causes the

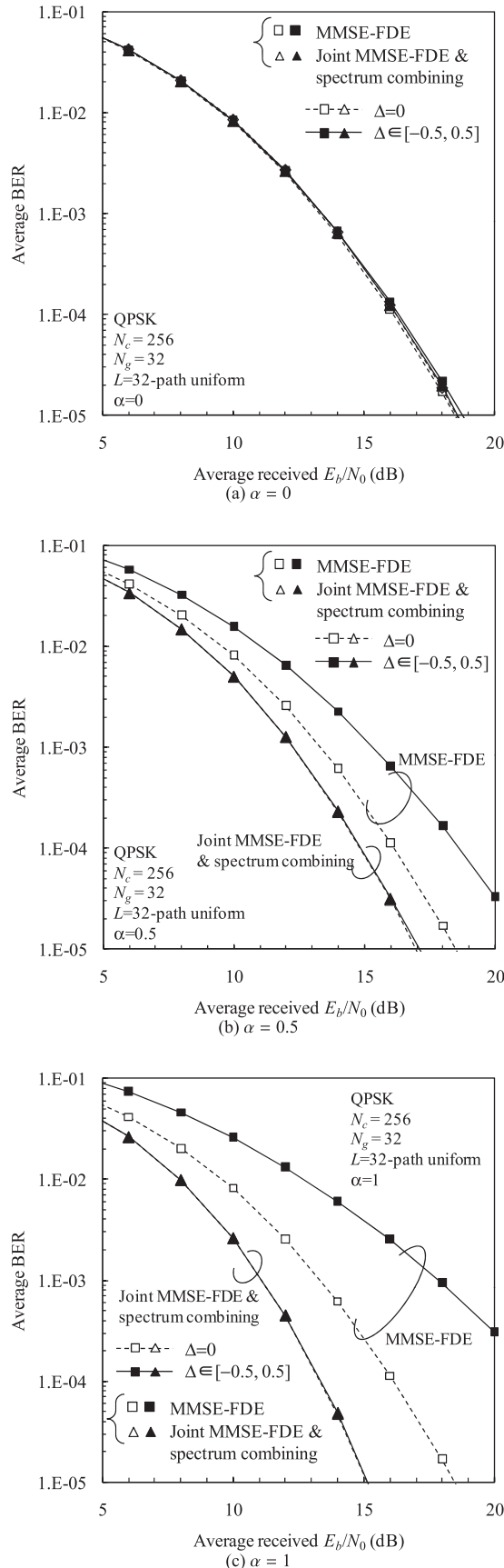


Fig. 10 BER performance.

BER performance degradation on the SC transmission using MMSE-FDE in the presence of timing offset. When the timing offset is present, the spectrum of the signal sampled at the symbol rate distorts since adjacent frequency-shifted spectra are given different phase rotations and they overlap if the roll-off factor of Nyquist filter is larger than 0. To solve this problem, we proposed a joint MMSE-FDE & spectrum combining. In the proposed joint MMSE-FDE & spectrum combining, the received signal is sampled at 2 times higher rate than the symbol rate to avoid overlapping of the adjacent frequency-shifted signal spectra and then, the simultaneous compensation of both the phase rotation caused by the timing offset and the spectrum distortion due to the channel frequency-selectivity and the spectrum combining based on MMSE criterion to restore the ISI-free condition over the desired frequency range are performed. We have shown by the computer simulation that the proposed joint MMSE-FDE & spectrum combining can provide almost the same BER performance as in the no timing offset case and furthermore, it can achieve better BER performance as the roll-off factor increases since the signal bandwidth becomes wider and therefore, larger frequency diversity gain can be achieved.

#### References

- [1] W.C. Jakes, Jr., ed., Microwave mobile communications, Wiley, New York, 1974.
- [2] J.G. Proakis, Digital communication, 4th ed., McGraw-Hill, 2001.
- [3] Y. Akaiwa, Introduction to digital mobile communication, Wiley, New York, 1997.
- [4] D. Falconer, S.L. Ariyavisitakul, A. Benyamin-Seeyar, and B. Eidson, "Frequency domain equalization for single-carrier broadband wireless systems," IEEE Commun. Mag., vol.40, no.40, pp.58–66, April 2002.
- [5] M.V. Clark, "Adaptive frequency-domain equalization and diversity combining for broadband wireless communications," IEEE J. Sel. Areas Commun., vol.16, no.8, pp.1385–1395, Oct. 1998.
- [6] F. Adachi, D. Garg, S. Takaoka, and K. Takeda, "Broadband CDMA techniques," IEEE Wireless Commun., vol.12, no.2, pp.8–18, April 2005.
- [7] F. Adachi and K. Takeda, "Bit error rate analysis of DS-SS with joint frequency-domain equalization and antenna diversity combining," IEICE Trans. Commun., vol.E87-B, no.10, pp.2991–3002, Oct. 2004.
- [8] L. Liu, C. Chen, and F. Adachi, "Impact of timing error on DS-SS with frequency-domain equalization," IEICE Technical Report, RCS2006-219, Jan. 2007.
- [9] T. Obara, H. Tomeba, K. Takeda, and F. Adachi, "Impact of timing offset on DS-SS with overlap FDE," 5th IEEE VTS Asia Pacific Wireless Communications Symposium (APWCS2008), Tohoku University, Sendai, Aug. 2008.
- [10] Y. Wang and X. Dong, "Comparison of frequency offset and timing offset effects on the performance of SC-FDE and OFDM Over UWB channels," IEEE Trans. Veh. Technol., vol.58, no.1, pp.242–250, Jan. 2009.
- [11] H. Tomeba, K. Takeda, and F. Adachi, "BER performance of single-carrier transmission with frequency-domain equalization in a channel having fractionally spaced time delays," Proc. 10th International Symposium on Wireless Multimedia Communications (WPMC), Jaipur, India, Dec. 2007.
- [12] H. Ando, M. Sawahashi, and F. Adachi, "Channel estimation filter using time-multiplexed pilot channel for coherent Rake combining



in DS-CDMA mobile radio,” IEICE Trans. Commun., vol.E81-B, no.7, pp.1517–1526, July 1998.

- [13] S. Takaoka and F. Adachi, “Pilot-aided adaptive prediction channel estimation in a frequency-nonsselective fading channel,” IEICE Trans. Commun., vol.E85-B, no.8, pp.1552–1560, Aug. 2002.
- [14] K. Takeda and F. Adachi, “Frequency-domain MMSE channel estimation for frequency-domain equalization of DS-CDMA signals,” IEICE Trans. Commun., vol.E90-B, no.7, pp.1746–1753, July 2007.
- [15] S. Okuyama, K. Takeda, and F. Adachi, “A study of frequency-domain filtering for SC-FDE,” IEICE Technical Report, RCS2009-27, June 2009.

## Appendix A: Derivation of Eq. (16)

$H(k, \Delta)$  of Eq. (12) can be rewritten as

$$H(k, \Delta) = \sum_{l'=-\infty}^{\infty} \sum_{l=0}^{L-1} h_l \int_{-\infty}^{\infty} \Phi(f) \exp j2\pi f(\Delta - \tau_l) \times \exp \left\{ -j2\pi \left( \frac{k}{N_c} - f \right) \right\} df, \quad (\text{A} \cdot 1)$$

where  $\Phi(f)$  is the transfer function of the overall (transmit+receive) filter, given by Eq. (19). Since

$$\sum_{n=-\infty}^{\infty} \exp(-j2\pi n f G) = \frac{1}{G} \sum_{n=-\infty}^{\infty} \delta \left( f - \frac{n}{G} \right), \quad (\text{A} \cdot 2)$$

where  $G$  is a positive real number, we obtain

$$H(k, \Delta) = \sum_{l'=-\infty}^{\infty} \sum_{l=0}^{L-1} h_l \exp \left\{ -j2\pi(k - l'N_c) \frac{\tau_l}{N_c} \right\} \Phi(k - l'N_c) \times \exp \left\{ j2\pi(k - l'N_c) \frac{\Delta}{N_c} \right\}. \quad (\text{A} \cdot 3)$$

Using

$$\sum_{l=0}^{L-1} h_l \exp \left\{ -j2\pi(k - l'N_c) \frac{\tau_l}{N_c} \right\} = H_c(k - l'N_c), \quad (\text{A} \cdot 4)$$

we finally obtain

$$H(k, \Delta) = \sum_{l'=-\infty}^{\infty} H_c(k - l'N_c) \Phi(k - l'N_c) \times \exp \left\{ j2\pi(k - l'N_c) \frac{\Delta}{N_c} \right\}. \quad (\text{A} \cdot 5)$$

## Appendix B: Derivation of the MMSE Weight for Joint MMSE-FDE & Spectrum Combining

Solving  $\partial E[|e(k)|^2] / \partial W(k - qN_c) = 0$  gives the MMSE weight  $\{W(k - qN_c); k = -N_c/2 \sim N_c/2 - 1, q = -1 \sim 1\}$ , where  $E[|e(k)|^2]$  is the MSE of the equalization error  $e(k)$ . Since

$$E[|e(k)|^2] = \frac{2E_s}{T_s} \left| \sum_{q=-1}^1 H(k - qN_c, \Delta) W(k - qN_c) - 1 \right|^2 + \sum_{q=-1}^1 E[|N(k - qN_c)|^2] W(k - qN_c) + \sum_{q=-1}^1 E[|\Pi(k - qN_c)|^2] W(k - qN_c), \quad (\text{A} \cdot 6)$$

we have

$$\frac{\partial E[|e(k)|^2]}{\partial W(k - qN_c)} = \frac{2E_s}{T_s} H(k - qN_c, \Delta) \left\{ \sum_{q=-1}^1 H^*(k - qN_c, \Delta) W^*(k - qN_c) - 1 \right\} + E[|N(k - qN_c)|^2 + |\Pi(k - qN_c)|^2] W^*(qN - k_c). \quad (\text{A} \cdot 7)$$

Solving  $\partial E[|e(k)|^2] / \partial W(k - qN_c) = 0$  and using  $\Lambda(k, \Delta) = (2E_s/T_s)/E[|N(k)|^2 + |\Pi(k)|^2]$ ,  $W(k)$  is given by Eq. (32).



**Tatsunori Obara** received his B.S. degree in Electrical, Information and Physics Engineering in 2008 and M.S. degree in communications engineering, in 2010, respectively, from Tohoku University, Sendai Japan. Currently he is a graduate student, studying toward his PhD degree at the Department of Electrical and Communications Engineering, Graduate School of Engineering, Tohoku University. His research interests include channel equalization techniques for mobile communication systems.



**Kazuki Takeda** received his B.S. and M.S. degrees in communications engineering from Tohoku University, Sendai, Japan, in 2006 and 2008. Currently he is a Japan Society for the Promotion of Science (JSPS) research fellow, studying toward his Ph.D. degree at the Department of Electrical and Communications Engineering, Graduate School of Engineering, Tohoku University. His research interests include precoding and channel equalization techniques for mobile communication systems. He

was a recipient of the 2010 IEICE RCS (Radio Communication Systems) Active Research Award.



**Fumiyuki Adachi** received the B.S. and Dr. Eng. degrees in electrical engineering from Tohoku University, Sendai, Japan, in 1973 and 1984, respectively. In April 1973, he joined the Electrical Communications Laboratories of Nippon Telegraph & Telephone Corporation (now NTT) and conducted various types of research related to digital cellular mobile communications. From July 1992 to December 1999, he was with NTT Mobile Communications Network, Inc. (now NTT DoCoMo, Inc.), where he

led a research group on wideband/broadband CDMA wireless access for IMT-2000 and beyond. Since January 2000, he has been with Tohoku University, Sendai, Japan, where he is a Professor of Electrical and Communication Engineering at the Graduate School of Engineering. His research interests are in CDMA wireless access techniques, equalization, transmit/receive antenna diversity, MIMO, adaptive transmission, and channel coding, with particular application to broadband wireless communications systems. From October 1984 to September 1985, he was a United Kingdom SERC Visiting Research Fellow in the Department of Electrical Engineering and Electronics at Liverpool University. He was a co-recipient of the IEICE Transactions best paper of the year award 1996 and again 1998 and also a recipient of Achievement award 2003. He is an IEEE Fellow and was a co-recipient of the IEEE Vehicular Technology Transactions best paper of the year award 1980 and again 1990 and also a recipient of Avant Garde award 2000. He was a recipient of Thomson Scientific Research Front Award 2004 and Ericsson Telecommunications Award 2008.